

Development of Multiplexed Analysis for the Photocatalytic

Activities of Nanoparticles in Aqueous Suspension

No Ah Lee^{a,c}, Soo Jin Kim^a, Bong-Jae Park^a, Hyun Min Park^b, Minjoong Yoon^{*c},
Bong Hyun Chung^d and Nam Woong Song^{*a}

^aCenter for Nanobio Convergence, Korea Research Institute of Standards and Science, 209
Gajeong-Ro, Yuseong-Gu, Daejeon 305-340, Rep. of Korea

^bCenter for Nano-Characterization, Korea Research Institute of Standards and Science,
Daejeon 305-340, South Korea

^cMolecular/Nano Photochemistry & Photonics Lab., Department of Chemistry, Chungnam
National University, 99 Daehak-Ro, Yuseong-Gu, Daejeon 305-764, Korea

^dBioNanotechnology Research Center, Korea Research Institute of Bioscience and
Biotechnology and Nanobiotechnology Major School of Engineering, University of Science
and Technology 111 Gwahang-Ro, Yuseong-Gu, Daejeon 305-806, Korea

*Corresponding authors:

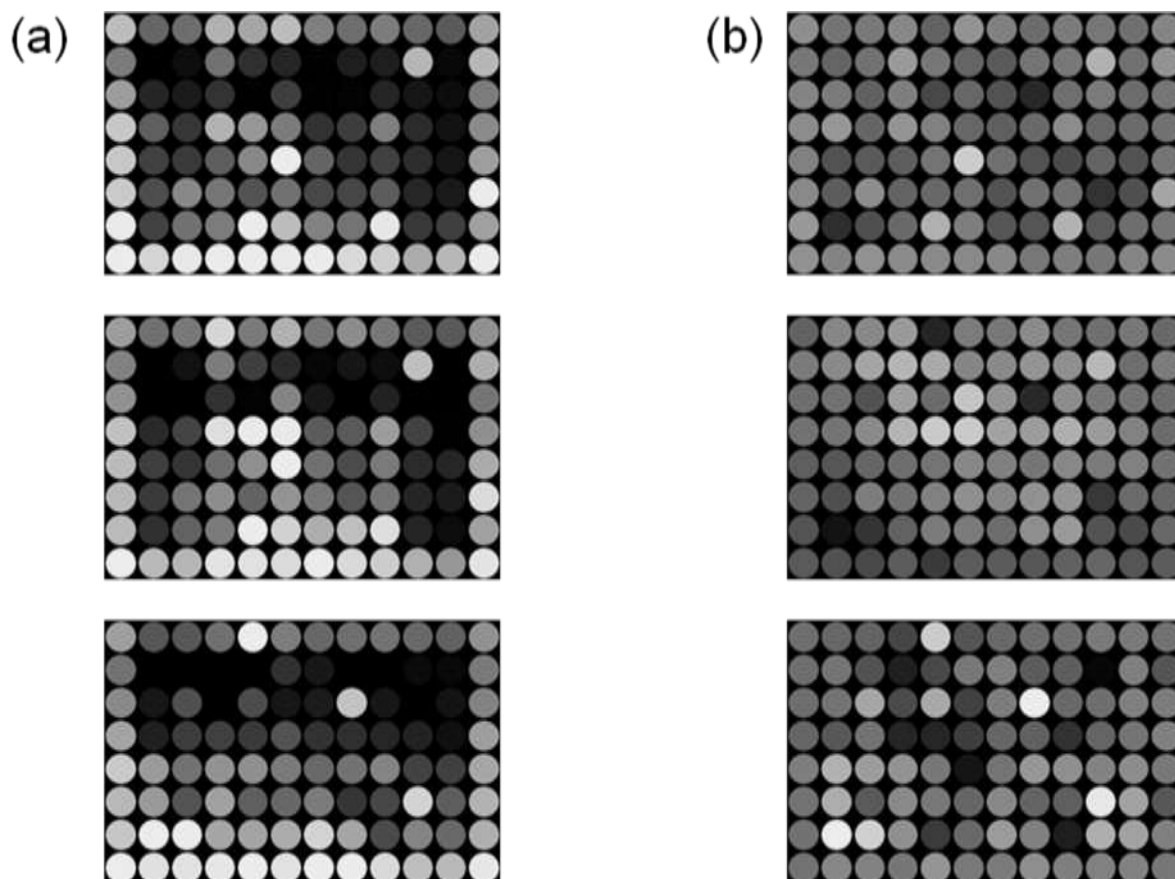
Nam Woong Song, Ph.D.

e-mail: nwsong@kriss.re.kr, Tel: +82-42-868-5214, Fax: +82-42-868-5032

Minjoong Yoon, Ph.D.

e-mail: mjyoon@cnu.ac.kr, Tel: +82-42-821-6546, Fax: +82-42-821-8896

Supporting Information



27

28

29 **Fig. S1.** (a) k_{app} values of NADH in each well depicted as a contrast image observed from
30 three independent plates. (A brighter circle corresponds to the well with higher rate constant)
31 (b) The reconstructed contrast image of the k_{app} 's corresponding to the images in the left
32 column. – Images in the first row are the same ones as in Fig. 2 in the main text.

33

34 ***S1. Experimental Parts***

35 ***S1.1 Materials***

36 TiO₂ as the photocatalytic nanomaterial was purchased from Evonic Co. LTD. (Aeroxide
37 Degussa P25[®]) and was used without further purification. To obtain a stable suspension of
38 TiO₂ NPs, 40 mg of TiO₂ powder was mixed into 10 mL of an aqueous NaOH (S8045, >98%,
39 Sigma-Aldrich) solution of pH 10 stored in a 20-mL glass vial ($\phi = 26$ mm). The solution was
40 stirred using a 22-mm magnetic bar at 900 rpm for 24 h and the suspension was maintained
41 for an additional 24 h without stirring to sediment large particles. Then 5 mL of the
42 supernatant was sampled for further analysis. The concentration of the TiO₂ NP suspension

43 was determined as 2.1 g/L by measuring the weight of the 1 mL of the suspension after
44 dehydration and comparing the UV absorbance at 310 nm with that of highly concentrated
45 suspensions. The hydrodynamic diameter of TiO₂ NPs in suspension was measured as 160 ~
46 190 nm using a particle size analyzer (ELS-Z, Otsuka electronics Co. Ltd.)

47 The stock solution of NADH for the PCA probe was prepared by dissolving 33 mg of
48 NADH (Cat. No. 43423 Fluka. Co. LTD.) into 10 mL of deionized water (DIW > 18 MΩ·cm⁻¹
49 ¹) obtained from the Milli-Q reference water system production unit (Millipore Co.). The
50 solution was then diluted by a factor of 5 ~ 80 to adjust the concentration adequately for the
51 experimental condition.

52 Acetic acid/sodium acetate, sodium phosphate monobasic/sodium phosphate dibasic
53 and sodium carbonate/sodium bicarbonate solutions of equal concentration were used for the
54 preparation of pH buffers of pH 5 ~ 6, pH 6 ~ 8 and pH 9 ~ 11, respectively. All of the
55 reagents for the preparation of pH buffers were purchased from Sigma-Aldrich as ACS
56 reagent grade.

57

58 ***S1.2 Spectral Measurement procedure***

59 Absorbance spectra of the TiO₂ suspension and NADH solution were recorded in the
60 wavelength range between 200 and 500 nm using a small-volume (100 μL) absorbance
61 cuvette (Hellma 105.201-QS) and a spectrophotometer (UV-1700, Shimadzu). The
62 fluorescence spectrum measurement of the NADH solution was carried out using a scanning-
63 type spectrofluorometer (Shimadzu RF-5301PC) with a small volume (100 μL) sample
64 cuvette (Hellma 105.250-QS).

65

66 ***S2. Dependence of NADH fluorescence intensity on NADH and TiO₂ concentrations***

67 To measure the oxidation rate of NADH by observing the fluorescence intensity, the

68 experiment should be performed in a concentration range exhibiting linear dependence of the
69 fluorescence intensity. The concentration dependence of the fluorescence intensity differs
70 according to the optical measurement geometry.¹ In this study, the top-read mode of
71 fluorescence microplate reader was used, which entail both excitation and detection of the
72 fluorescence through optical fibers located above a 96-well plate. In this optical geometry, the
73 fluorescence intensity of NADH showed a linear dependence on NADH concentration up to
74 250 μM with a coefficient of determination close to 1 ($R^2 = 0.995$) (Table S1 and Fig. S2(a)).
75 The fluorescence intensity exhibited saturation behaviour when the concentration was
76 increased over 125 μM . Similar dependence of the NADH fluorescence intensity on the
77 concentration could be observed in the presence of TiO_2 NPs (Table S1 and Fig. S2(b)). Such
78 behaviour is due to the absorption of excitation light in the direction of propagation. Because
79 the conjugate focal point of the detection fiber input lies at a certain depth within the NADH
80 solution, the excitation light reaching that point is more attenuated by the absorption of
81 NADH as the concentration increases. Based on these results, the maximum concentration of
82 NADH was set to 125 μM .

83

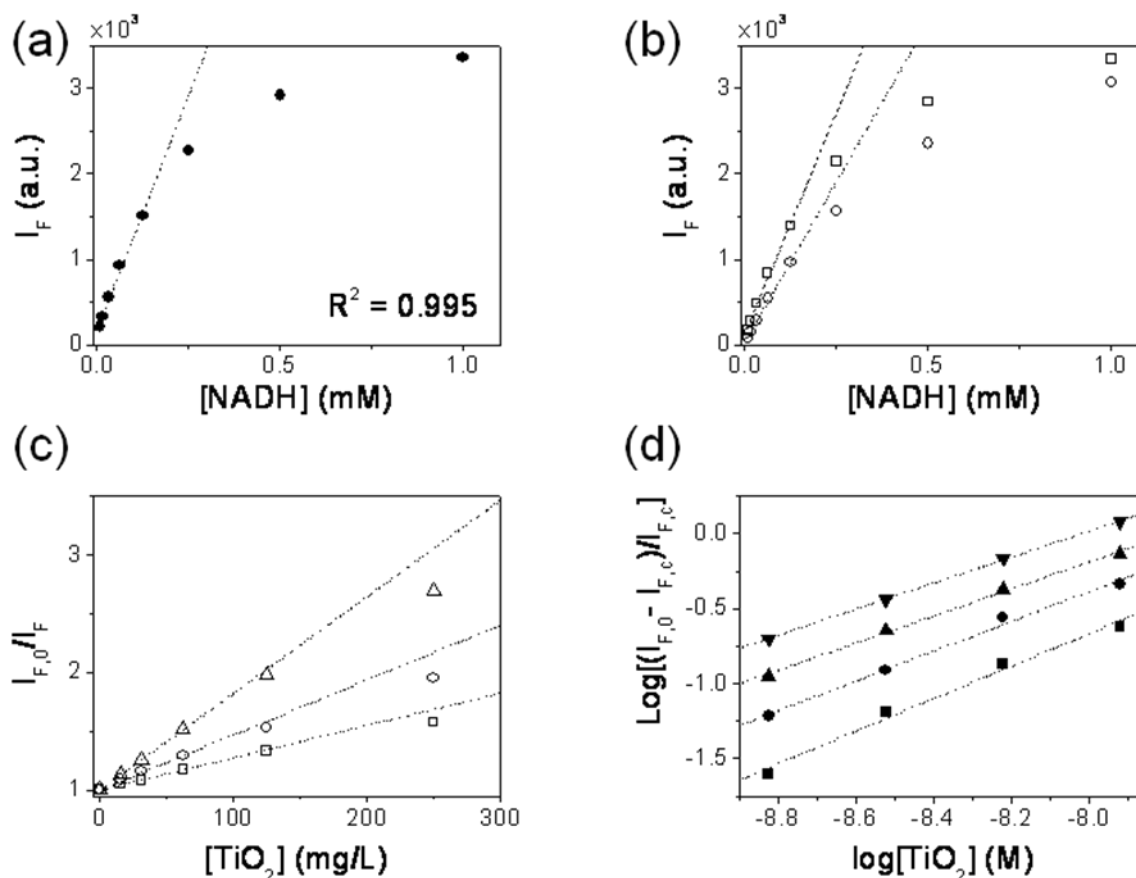
84 **Table S1** Fluorescence intensities of NADH observed at various concentrations of NADH
85 and TiO_2 NPs

[NADH] (μM)	[TiO_2] (mg/L)					
	0	16	31.3	62.5	125	250
7.82	212.0	186.8	169.3	139.8	106.8	78.75
15.6	326.6	294.3	272.3	239.1	193.8	148.4
31.3	556.3	509.8	479.7	428.9	364.1	285.1
62.5	931.4	869.8	837.3	758.8	654.6	535.1
125	1,510	1,428	1,391	1,284	1,130	958.5
250	2,276	2,186	2,145	2,026	1,785	1,558
500	2,919	2,877	2,848	2,741	2,572	2,353
1,000	3,366	3,337	3,342	3,305	3,228	3,071

86 * pH value was adjusted to 8 with 5 mM phosphate buffer

87

88



89

90 **Fig. S2.** (a) The dependence of fluorescence intensity on NADH concentration in the absence
 91 of TiO₂ NPs. (b) The dependence of the NADH fluorescence intensity on NADH
 92 concentration in the presence of TiO₂ NPs of (\square) 31.3 and (\circ) 250 mg/L. (c) The dependence
 93 of NADH fluorescence intensity on the concentration of TiO₂ NPs with NADH concentration
 94 of (\square) 125, (\circ) 31.3 and (\triangle) 7.82 μ M. (d) The plot of $\text{log} [(I_{F,0} - I_{F,c})/I_{F,c}]$ vs. $\text{log} [\text{TiO}_2]$. ($I_{F,0}$: I_F
 95 w/o TiO₂; $I_{F,c}$: I_F at TiO₂ concentration of c with I_F ; NADH fluorescence intensity at 460 nm).
 96

97 The presence of TiO₂ NPs in solution resulted in a decrease of NADH fluorescence
 98 intensity, most likely due to charge transfer quenching from the photoexcited NADH to the
 99 TiO₂ NP surface.^{2, 3} Because the fluorescence intensity of the NADH/TiO₂ suspension was
 100 constant over time without UV irradiation, the reduction in fluorescence intensity after the
 101 addition of TiO₂ NPs could not be due to the catalytic decomposition of NADH in the dark.
 102 The Stern-Volmer plot of the NADH fluorescence intensity vs. TiO₂ concentration showed a
 103 linear relationship when the TiO₂ was present in the concentration range of 3.9 ~ 62.5 mg/L

104 (Fig. S2(c)). Negative deviations from the linear regression line were observed when the TiO₂
105 concentration was increased above 62.5 mg/L. Such behaviour is usually observed when the
106 fluorescence quenching is accompanied by quencher binding.^{3,4} In this case, it is possible to
107 deduce the binding constant of NADH to the TiO₂ surface from the intercept of the linear
108 regression as $K_a \sim 2.5 \times 10^7 \text{ M}^{-1}$ according to Eqn (S1) (Fig. S2(d)).³

$$109 \quad \log \left[\frac{I_{F,0} - I_{F,c}}{I_{F,c}} \right] = \log K_a + n \log [\text{TiO}_2] \quad (\text{S1})$$

110

111 ***S3. Dependence of the NADH photo-oxidation rate on NADH and TiO₂ concentrations***

112 The dependence of the NADH photo-oxidation rate on the TiO₂ concentration at various
113 NADH concentrations has been summarized in Table S2 and Fig. S3(a). The apparent rate
114 constant, k_{app} , could be obtained from the linear regression for the relative fluorescence
115 intensity vs. UV irradiation time. The k_{app} values were linearly dependent on the TiO₂
116 concentration in the range of 3.9 ~ 31.3 mg/L regardless of the NADH concentration in the
117 range of 31 ~ 250 μM. When the TiO₂ concentration was lower than 3.9 mg/L, the PCA of
118 suspended TiO₂ NP was too small to allow observation of the reaction rate with low relative
119 uncertainty. On the other hand, when the TiO₂ concentration was higher than 31.3 mg/L,
120 saturation behaviour was observed due to the absorption and scattering of UV light by TiO₂
121 NPs. To obtain consistent PCA values, the measurement should be performed under the
122 experimental conditions that show linear dependence of k_{app} values on the TiO₂ concentration.
123 In our experiment, k_{app} values showed linear dependence on the TiO₂ concentration when
124 TiO₂ suspension was prepared with a transmittance between 3.2×10^{-2} and 0.72 (0.15 ~ 1.5 in
125 optical density) at 312 nm measured using a cell with 1-cm path length.

126

127

128 **Table S2** Photo-oxidation rate constant (k_{app})^a of NADH in the presence of TiO₂ NPs

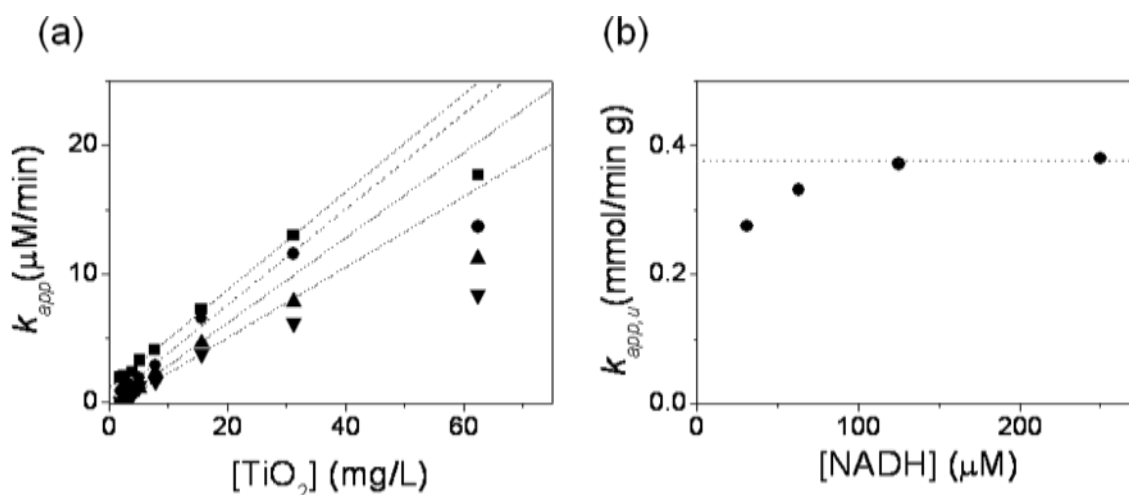
[TiO ₂] (mg/L)	[NADH] (μM)			
	31.3	62.5	125	250
1.96	0.05	0.27	0.93	1.96
2.61	0.13	0.31	1.29	2.04
3.91	0.51	0.84	1.32	2.41
5.21	1.30	1.15	1.96	3.30
7.82	1.61	2.34	2.89	4.08
15.7	3.80	4.68	6.53	7.24
31.3	6.17	7.87	11.6	13.0
62.5	8.40	11.2	13.7	17.7
125	7.92	14.2	15.1	21.0

129 ^a The unit of k_{app} is μM/min.

130 * pH value was adjusted to 8 with 5 mM phosphate buffer

131

132



133

134 **Fig. S3.** (a) The dependence of k_{app} values on TiO₂ concentration. The concentration of
135 NADH was (■) 250, (●) 125, (▲) 62.5 and (▼) 31.3 μM, respectively. (b) The dependence
136 of the TiO₂-normalized apparent rate constant on the NADH concentration.

137

138 The slope in the linear range of k_{app} vs. TiO₂ concentration gives the normalized value
139 of the apparent reaction rate constant, $k_{app,u}$, with respect to TiO₂ concentration. As shown in
140 Fig. S3(b), the value of $k_{app,u}$ changed with the concentration of NADH.

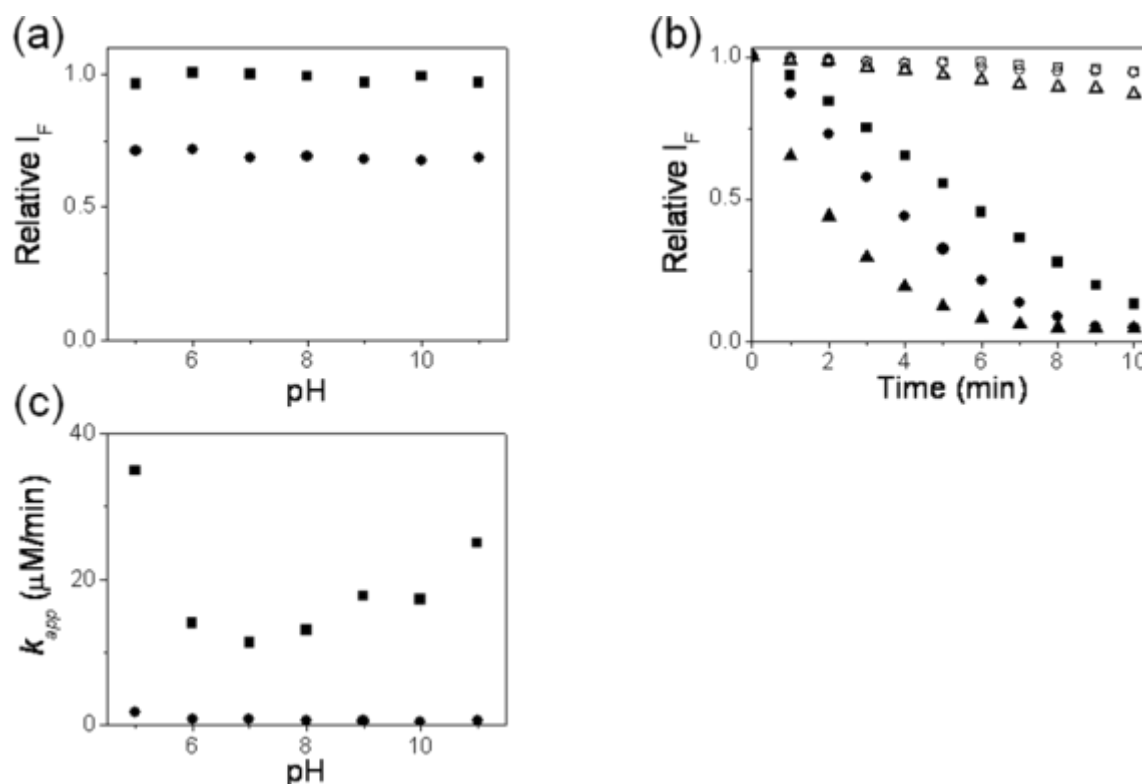
141 An increase of *ca.* 35% in $k_{app,u}$ value could be observed when NADH concentration
142 was increased from 35 to 125 μM. The variation of $k_{app,u}$ value was observed to fall within
143 2.5% at the concentrations of 125 and 250 μM. Thus it is preferred to perform PCA analysis

144 in the NADH concentration range of 125 ~ 250 μM , where consistent values of $k_{app,u}$ can be
145 obtained to minimize the concentration effect of the substrate. From the above results, proper
146 concentrations of the substrate and photocatalyst could be determined with regard to the
147 linearity of the fluorescence intensity and the reaction rate.

148

149 **S4. pH dependence of NADH photo-oxidation rate**

150 It has been reported that the substrate degradation by PCA is dependent on the pH of the
151 suspension.^{5,6} We determined the photo-oxidation rate of NADH in the presence of TiO_2 at
152 various pH values by monitoring the reaction in pH buffered suspensions. The pH of the
153 suspensions was varied from 5 to 11 with interval of pH 1.



154 **Fig. S4.** (a) Relative fluorescence intensities of NADH normalized by the intensity of a pH 7
155 NADH solution (125 μM) in the absence (\blacksquare) and presence (\bullet) of TiO_2 NPs. (b) The decrease
156 in the relative fluorescence intensity as a function of UV irradiation time in the absence (open
157 symbol) and presence (closed symbols) of TiO_2 NPs at various pH values. (Δ , \blacktriangle) at pH 5, (\square ,
158 \blacksquare) at pH 7, and (\circ , \bullet) at pH 10. (c) The dependence of the NADH photo-oxidation rate on the
159 suspension pH in the absence (\bullet) and presence of (\blacksquare) TiO_2 NPs.

160

162 **Table S3** pH dependence of photo-oxidation rate constants

pH	Photo-oxidation rate constant ^a (k_{app})	
	NADH only	with TiO ₂
5	1.70	35.0
6	0.846	14.0
7	0.754	11.3
8	0.654	13.1
9	0.500	17.7
10	0.476	17.3
11	0.648	25.0

163 ^aThe unit of k_{app} is $\mu\text{M}/\text{min}$.
164

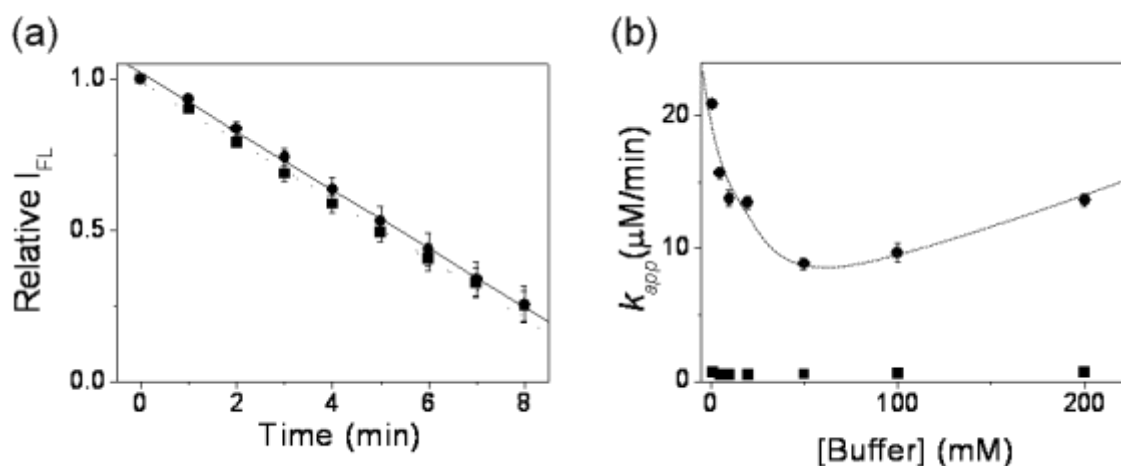
165 The fluorescence spectrum of NADH was not altered by the change of pH in the
166 range of pH 5 and pH 11. The degree of NADH fluorescence quenching by TiO₂ was also
167 similar in the pH range of interest (Fig. S4(a)). This result shows that the NADH adsorption
168 to the TiO₂ surface was not influenced by the pH of the suspension. The photo-oxidation rate
169 of NADH without TiO₂ in solution slightly decreased from pH 5 to pH 10 exhibiting a very
170 low rate constant and the rate increased again at pH 11 (Table S3 and Fig. S4(b)). However,
171 the photo-oxidation rate of NADH in the presence of TiO₂ was greatly altered by the pH
172 change in the suspension. The k_{app} value was modulated up to 3 fold during the pH change of
173 the suspension from pH 5 (acidic) to pH 11 (basic) (Fig. S4(c)). Therefore, it is noted that the
174 suspension pH should be defined using pH-buffered suspensions in the PCA analysis to
175 obtain consistent results.
176

177 ***S5. The dependence of NADH photo-oxidation rate on pH buffer ions***

178 We also observed an effect of the composition or the concentration of buffer ions on
179 the PCA measurement. The photo-oxidation rate was not altered when the composition of the
180 buffer ions was changed, but it was dependent on the concentration of the ions. When we
181 performed PCA analysis in acetate and phosphate buffers of pH 6, the results agreed within
182 0.7% (Fig. S5(a)). On the other hand, the photo-oxidation rate was modulated more than 2

183 fold by the change in the phosphate ion concentration at pH 8 (Fig. S5b). The reaction rate
184 was decreased when the buffer concentration was increased from 1 to 50 mM and it increased
185 again with an increase in the buffer concentration from 50 to 200 mM. From the above results,
186 it is suggested that the buffer concentration and the pH of the suspension should be held in
187 constant in the measurement of PCA using NADH photo-oxidation.

188



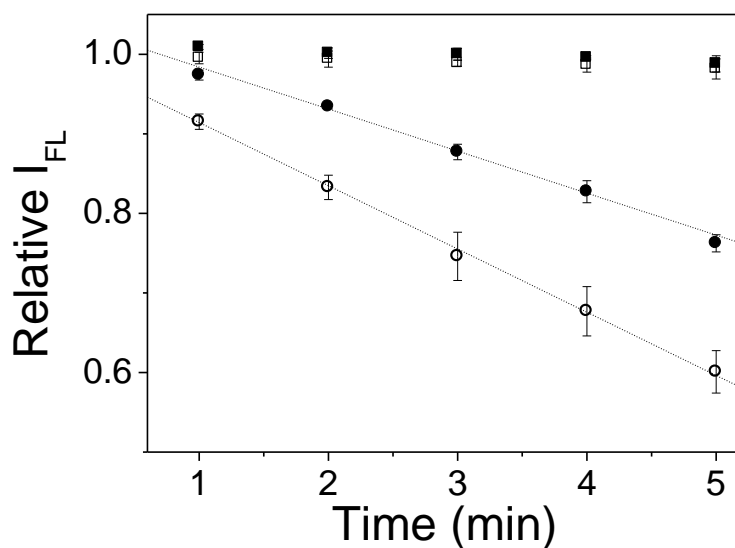
189

190 Fig. S5. (a) The decrease in the relative fluorescence intensity of NADH as a function of the
191 UV irradiation time in the presence of TiO_2 NPs at pH 6 adjusted using acetate (■) or
192 phosphate (●) buffer. (b) The dependence of the NADH photo-oxidation rate on the
193 concentration of pH buffer ions in the absence (■) and presence (●) of TiO_2 NPs. (The dashed
194 line is a simple auxiliary line for the presentation of tendency)

195

196 **S6. Photo-oxidation kinetics of NADH in the presence of TiO_2 NPs**

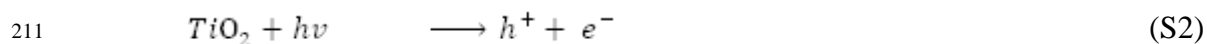
197 The photo-oxidation rate of NADH becomes higher in the presence of TiO_2 NPs because
198 various kinds of radicals and ROS can be generated on the surface of the NPs. The
199 participation of ROS generated on the TiO_2 surface in the photocatalytic oxidation of NADH
200 could be observed through the PCA assay in the presence of ethanol, which is known to be a
201 hydroxyl-radical scavenger.⁷ The photo-oxidation rate of NADH in the presence of TiO_2 was
202 reduced by 34 % when 2.5 mM ethanol was added (Fig. S6).



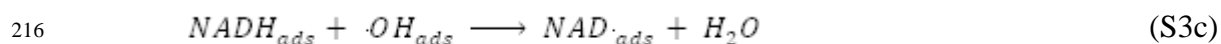
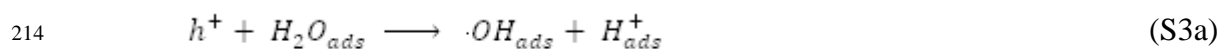
203

204 **Fig. S6.** The decrease in the relative fluorescence intensity as a function of UV irradiation
 205 time in the absence (open symbol) and presence (closed symbols) of 2 mM ethanol as the
 206 radical scavenger. (□, ■) 125 μM NADH solution, (○, ●) 125 μM NADH and 100 mg/L TiO₂
 207 suspension.
 208

209 When UV light is applied, holes (h^+) and electrons (e^-) are generated on the surface
 210 of TiO₂ as a result of photocatalytic activation.



212 Holes and electrons generate hydroxyl-radical or superoxide by reaction with water,
 213 hydroxide ion, or adsorbed molecular oxygen to oxidize NADH.^{5, 8-11}



219 Here, the subscript 'ads' indicates the species adsorbed on the surface of TiO₂ NPs.

220 The dependence of the NADH photo-oxidation rate on the suspension pH can be
221 explained by the above suggested reaction mechanisms. In the suspension of pH 7, ROS are
222 generated *via* the reactions in Eqns (S3a) and (S4a); however, ·OH generation becomes more
223 effective in basic suspensions (pH > 7) through the reaction in Eqn (S3b). This process was
224 expressed as an increased rate of NADH photo-oxidation along with the increase of
225 suspension pH. On the other hand, the reaction of NADH with O_2^- in Eqn (S4b) becomes
226 faster in acidic suspensions (pH < 7) due to the increased concentration of the adsorbed
227 aqueous protons (Fig. S4(c)).

228

229 References for Supporting Information

- 230 1. J. R. Lakowicz, *Principles of Fluorescence Spectroscopy*, Springer, New York, 1999.
- 231 2. W. J. E. Beek and R. A. J. Janssen, Photoinduced electron transfer in
232 heterosupramolecular assemblies of TiO₂ nanoparticles and terthiophene carboxylic
233 acid in apolar solvents, *Adv. Funct. Mater.*, 2002, **12**, 519-525.
- 234 3. A. Kathiravan and R. Renganathan, Interaction of colloidal TiO₂ with bovine serum
235 albumin: A fluorescence quenching study, *Colloid Surface A*, 2008, **324**, 176-180.
- 236 4. C. M. Samworth, M. D. Esposti and G. Lenaz, Quenching of the intrinsic tryptophan
237 fluorescence of mitochondrial ubiquinol—cytochrome-c reductase by the binding of
238 ubiquinone, *Eur. J. Biochem.*, 1988, **171**, 81-86.
- 239 5. N. Daneshvar, M. Rabbani, N. Modirshahla and M. A. Behnajady, Kinetic modeling
240 of photocatalytic degradation of Acid Red 27 in UV/TiO₂ process, *J. Photochem.*
241 *Photobiol. A: Chem.*, 2004, **168**, 39-45.
- 242 6. A. R. Rahmani, M. T. Samadi and A. Enayati Moafagh, Investigation of
243 photocatalytic degradation of phenol by UV/TiO₂ process in aquatic solutions, *J. Res.*
244 *Health Sci.*, 2008.
- 245 7. M. Suthanthiran, S. D. Solomon, P. S. Williams, A. L. Rubin, A. Novogrodsky and K.
246 H. Stenzel, Hydroxyl radical scavengers inhibit human natural killer cell activity,
247 *Nature*, 1984, **307**, 276-278.
- 248 8. T. Daimon and Y. Nosaka, Formation and behavior of singlet molecular oxygen in
249 TiO₂ photocatalysis studied by detection of near-infrared phosphorescence, *J. Phys.*
250 *Chem. C*, 2007, **111**, 4420-4424.
- 251 9. K.-i. Ishibashi, A. Fujishima, T. Watanabe and K. Hashimoto, Generation and
252 deactivation processes of superoxide formed on TiO₂ film illuminated by very weak
253 UV light in air or water, *J. Phys. Chem. B*, 2000, **104**, 4934-4938.
- 254 10. T. A. Konovalova, J. Lawrence and L. D. Kispert, Generation of superoxide anion and
255 most likely singlet oxygen in irradiated TiO₂ nanoparticles modified by carotenoids, *J.*
256 *Photochem. Photobiol. A: Chem.*, 2004, **162**, 1-8.
- 257 11. S. Xu, J. Shen, S. Chen, M. Zhang and T. Shen, Active oxygen species (1O_2 , $O_2^{\cdot-}$)
258 generation in the system of TiO₂ colloid sensitized by hypocrellin B, *J. Photochem.*
259 *Photobiol. B: Biol.*, 2002, **67**, 64-70.